Ferroelectric nanodomains in the uniaxial relaxor system $Sr_{0.61-x}Ba_{0.39}Nb_2O_6:Ce_x^{3+}$

P. Lehnen and W. Kleemann
Laboratorium für Angewandte Physik, Gerhard Mercator Universität, D-47048 Duisburg, Germany

Th. Woike
Institut für Mineralogie, Universität zu Köln, D-50674 Köln, Germany

R. Pankrath
Fachbereich Physik, Universität Osnabrück, D-49069 Osnabrück, Germany
(Received 30 March 2001; published 21 November 2001)

The domain morphology of the disordered relaxor ferroelectric strontium barium niobate doped with cerium, $Sr_{0.61-x}Ba_{0.39}Nb_2O_6:Ce_x^{3+}$, has been investigated by piezoelectric force microscopy. The evolution of natural and written domains above the phase-transition temperature T_C reveals a very slow relaxation into a depolarized multicluster state. This hints at strong pinning forces due to quenched random fields. Below T_C zero-field-cooled nanodomains are observed to show fractal-like shapes. Their size distribution can be described by a power law with exponential cutoff in accordance with the random-field Ising model.

DOI: 10.1103/PhysRevB.64.224109 PACS number(s): 68.37.Ef, 77.80.Dj, 77.80.Fm

I. INTRODUCTION

Relaxor ferroelectrics are characterized[1] by (i) a significant frequency dependence of their peak permittivity, (ii) persistence of the local polarization far above the phase-transition temperature T_C, and (iii) absence of macroscopic spontaneous polarization and structural symmetry breaking after zero-field cooling. Relaxor ferroelectric behavior occurs dominantly in lead based perovskite structures of $A(B_1B_2)O_3$ compositions. The archetypical relaxor compound is the disordered $PbMg_{1/3}Nb_{2/3}O_3$ (PMN) discovered by Smolenskii *et al.*[2] Similar features are also observed on tungsten bronze-structure materials such as $A_xBa_{1-x}Nb_2O_6$ ($A=$Sr, Pb).[3]

Superparaelectric[1] and dipolar glass models[4] have been proposed to explain the polar dynamics and their extreme slowing down at the ''diffuse'' phase transition. However, these models are not capable of describing the ferroelectric symmetry breaking on a nanometric scale.[5] A spherical cluster glass model[6] involving both random bonds and quenched random fields has recently proposed to describe essential properties of PMN type relaxors both above and below T_C leaving open, however, the mechanism of nanocluster formation. Their occurrence in the paraelectric phase is meanwhile accepted to be at the heart of the relaxor properties.[7,8] Their origin is very likely explained by a random-field (RF) mechanism[9–11] as a consequence of local-charge disorder.

The present research on the disordered uniaxial relaxor compound $Sr_{0.61}Ba_{0.39}Nb_2O_6$ (SBN) is motivated by the need to reduce the number of degrees of freedom to come closer to a simple model situation. Indeed, recent results of the dielectric susceptibility dispersion[12] and linear birefringence measurements[13,14] have shown that $Sr_{0.61-x}Ba_{0.39}Nb_2O_6:Ce_x^{3+}$ (SBN:Ce) belongs to the same universality class as the three-dimensional random-field Ising model (3D RFIM). Especially the observed crossover of the critical exponents γ and ν from 3D Ising to 3D RFIM behavior upon increasing the doping with Ce^{3+} confirms that charge disorder is at the origin of the postulated RF's.[13,14]

As another consequence of the quenched RF's one expects[11,15] extreme critical slowing down upon cooling towards T_C and breaking into a ferroelectric domain state below T_C. In this paper, we report on direct evidence of the polar nanodomains using piezoelectric force microscopy (PFM) under high-resolution conditions. This technique is adequate for viewing spontaneous and relaxing domains on a nanoscale, which is out of reach for the noncontact atomic-force technique used previously[16] to monitor the ferroelectric switching process in SBN:Ce. Further, the thermal instability of poled macrodomains is investigated by studying the appearance of surface roughness at $T<T_C$ and their temporal decay into nanoclusters at $T>T_C$.

II. EXPERIMENTAL PROCEDURE

Ce_x ($x=0.0113$) doped SBN crystals were grown by the Czochralski technique. Platelet-shaped samples of approximately 0.1 mm thickness with the polar c axis ([001] direction) perpendicular to the surface were cut and polished to optical quality.

Domain images were obtained with a commercial atomic-force microscope (TOPOMETRIX™, Explorer)[17] operating in PFM mode.[18] The PFM is a voltage-modulated contact method,[19,20] where an ac voltage $V_{ac}=V_0\sin\omega t$ with an amplitude $V_0=10-20$ V and a frequency $\omega=9.3$ kHz is applied between the tip and the bottom electrode of the sample.[18,21] Due to the converse piezoelectric effect the alternating external field gives rise to a sinusoidal thickness variation of the ferroelectric sample. This can be measured via the oscillation of the cantilever while phase shifts of 0° and 180°, respectively, are directly related to antiparallel (180°) domains. V_0 is chosen to be large enough for a reasonable signal-to-noise ratio, but well below the switching threshold.

Two kinds of cantilevers were used. One is the standard platinum-coated cantilever for electrostatic-force microscopy from TOPOMETRIX™ having a resonance frequency of ap-

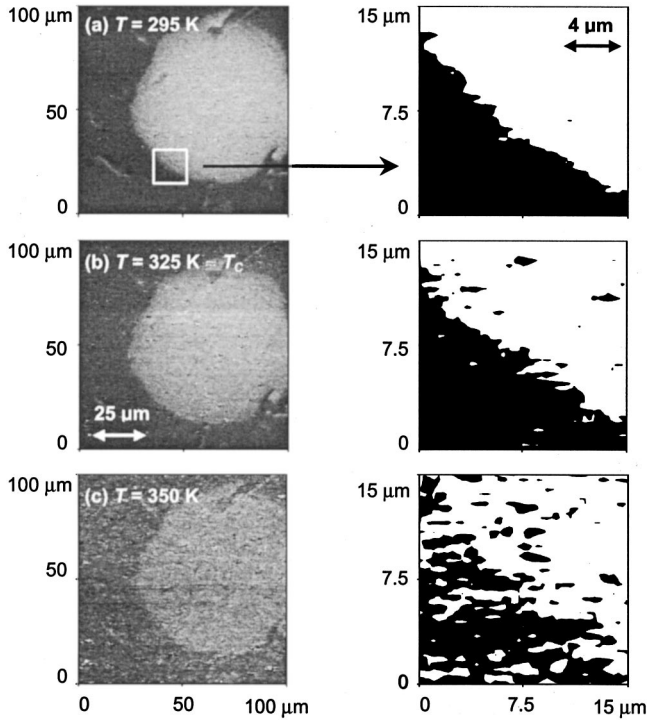

FIG. 1. Natural 180° domain polarized downward in an upward directed (or neutral) environment at temperatures $T=295$ K (a), 325 K (b), and 350 K (c) in full size (left column) and magnified (right column) in order to present details of the domain boundary in binary contrast.

proximately 90 kHz and a nominal spring constant of 2–4.5 Nm^{-1}. The other cantilever from NANOSENSORS™ has a spring constant of 0.18 Nm^{-1} and a resonant frequency of 12 kHz. It was used for the high-resolution scans. Ferroelectric domain writing processes were performed by applying a static voltage, $V_{\mathrm{dc}}=\pm 80$ V, to the conductive tip, while it was dragged in contact over the sample surface at a speed of 25 μm/s. Temperatures between 290 K and 350 K were achieved using a self-built hot stage. The temperatures were measured with a NiCr-Ni thermocouple to within an accuracy of 0.5 K.

III. RESULTS AND DISCUSSION

Figure 1 shows the thermal evolution of a macroscopic 180° domain (left column) upon heating from $T=295$ K up to 350 K. This domain is a left over of a preceding poling process. Its polarization is downward directed in an upward directed or neutral environment. The right column presents the magnified rim of the domain. Below $T_C \approx 320$ K the domain wall[13] is rather smooth and well defined. On heating to above T_C one observes a gradual roughening of the domain wall. Both, the domain and the environment decay into small isolated polar clusters of either sign on a submicron scale. Furthermore, the contrast (i.e., the difference in the average polarization values) between the domain and its environment gradually fades out at $T>T_C$, but surprisingly persists up to $T=350$ K. This contrasts with the behavior of a normal ferroelectric material and hints at a local memory of the

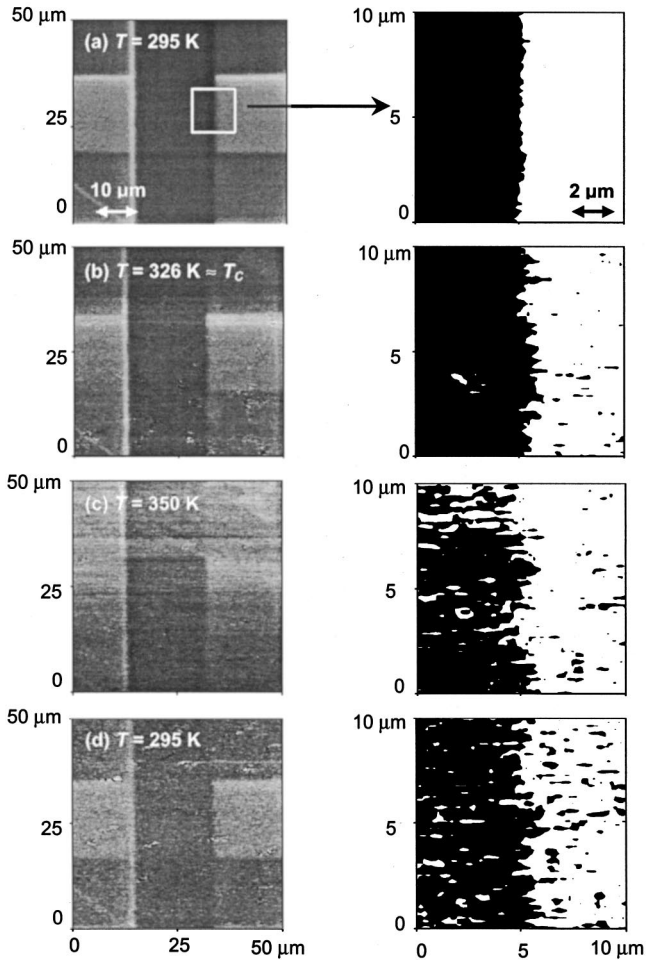

FIG. 2. Checked 180° domain structure written with ±80 V at temperatures $295\ \mathrm{K}<T<350$ K (a)–(d) (see text). The right column presents a magnified square section as indicated in binary contrast.

symmetry-broken phase. It reflects the fluctuations of the quenched RF's conserved in the high-temperature relaxor phase.

Similar temperature-induced roughening of the domain walls can be observed in written domains as displayed in Fig. 2. The checked domain structure in Fig. 2(a) (left column) was obtained by first homogeneous writing at $T=295$ K with −80 V applied to the tip. In a second step the central horizontal and, finally, the central vertical stripe were written with +80 V and −80 V applied to the tip, respectively. Figure 2(b)–2(d) shows the same section as in Fig. 2(a) at elevated temperatures, $T=326\ \mathrm{K}\approx T_C$ (b) 350 K (c), and recooled to 295 K (d). The right column of Fig. 2 presents the magnified domain pattern out of a square section as indicated on the left column in binary contrast. As already seen in Fig. 1 the domain-wall roughens when heating to temperatures $T>T_C$ and the domains decay into polar clusters. However, the written domain structure is not completely deleted even at temperatures $T\approx T_C+30$ K. Obviously the decay into the paraelectric phase is hampered by the local pinning forces of the quenched RF's counteracting the establishment of paraelectric disorder. As will be outlined below, these pin-

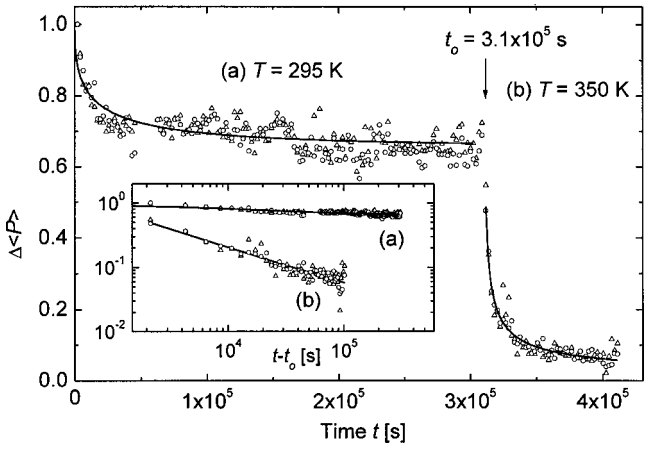

FIG. 3. Isothermal relaxation of the averaged polarization contrast, $\Delta\langle P\rangle$, after writing at $T=295\,\mathrm{K}$ (a) and heating to $T=350\,\mathrm{K}$ (b) in forward (triangles) and reverse (circles) scan direction, respectively. The inset shows double-logarithmic plots with fits to (a) stretched exponential and (b) power laws, respectively (solid lines, see text), where $t_0=0$ (a) and 3.1×10^5 s (b).

ning forces give rise to extremely sluggish dynamics even in the paraelectric regime.

Cooling the sample again to below T_C one observes a coarse graining of the randomly distributed up and down domains [Fig. 2(d)]. These nanodomains appear at those places where the underlying spatial RF fluctuations favor the formation of an inverted domain despite the unfavorable increase of the free energy due to domain-wall formation. Nevertheless, the emerging macroscopic ferroelectric domain structure still comes close to the initial one.

In a normal ferroelectric material the domains are expected to be static below the phase-transition temperature and to decay rapidly above T_C. However, in SBN:Ce very strong pinning forces due to the quenched RF's are active, which give rise to decelerated dynamics in both the ferroelectric and in the paraelectric phase. Figure 3 shows the temporal relaxation of the difference of the average polarization (difference in contrast after fast-Fourier transformation), $\Delta\langle P\rangle=\langle P_\downarrow\rangle-\langle P_\uparrow\rangle$, of written upward and downward polarized domains (cf. Fig. 2) at two different temperatures in the ferroelectric (a) and in the paraelectric regime (b), respectively. At $T=295\,\mathrm{K}$ the remanence stabilizes at about 65% of the saturated initial value within a time of about 4×10^4 s. This relaxation is well described by a Kohlrausch-Williams-Watts (KWW) stretched exponential decay, $\Delta\langle P\rangle=(P_0-P_\infty)\exp[-(t/\tau)^\beta]+P_\infty$ with $\tau=16340\pm3160\,\mathrm{s}$, $\beta=0.45\pm0.07$, and $P_\infty=0.66\pm0.01$ (solid line in Fig. 3), while $P_0=1$ by data normalization. Obviously relaxation into a ''quasistatic'' domain state is encountered, which is considered as the result of microscopical backswitching processes. One has to take into account that the initially written domains exist only in the vicinity of the crystal surface owing to the decrease of the applied electric field far from the tip.[22] In the volume of the crystal, where the writing field falls below the coercive field of 140 kV/m,[23] the original domain structure resists the writing process. Backswitching will take place primarily at the interface between the superficial single domain and the bulk polydomains. Here the formation of nanodomains is supported by the underlying spatial RF fluctuations. Another mechanism is due to depolarizing stray fields at the surface. Since the tip is in contact with the surface, no polarization compensating charges exist. Therefore, stray fields due to the written domain structure give rise to depolarization at the surface. Both effects support the formation of nanodomains leading to a broad distribution of domain sizes and, consequently, activation energies. The resulting polydispersivity is reflected by the small β value. We have to mention that these data can also be fitted with a power law, $\Delta\langle P\rangle=P_\infty+P_0(t-t_0)^{-\beta}$ with $P_0=11.3\pm7.0$, $P_\infty=0.63\pm0.02$, $\beta=0.45\pm0.08$, and the starting time $t_0=0$. The fit (not shown) is of the same quality as, but indistinguishable from the KWW fit shown in Fig. 3. Unfortunately there is presently no theoretical approach describing the dynamics of backswitching processes under the constraint of RF's. Here we prefer phenomenologically the KWW description, which avoids an unphysical divergence of $\Delta\langle P\rangle$ at $t=0$.

After reaching quasiequilibrium at $T=295\,\mathrm{K}$ and rapidly heating to $T=350\,\mathrm{K}\approx T_C+30\,\mathrm{K}$ a very slow decay into a depolarized state is observed. It is well described by a power law, $\Delta\langle P\rangle=P_\infty+P_0(t-t_0)^{-\beta}$ with $\beta=0.57\pm0.05$, $P_0=39.6\pm13.9$, and $P_\infty\approx0$, where $t_0=3.1\times10^5$ s is the starting time [solid line (b) in Fig. 3]. A similar fractal time dependence was observed on the magnetization of RF-induced metastable domains in the diluted antiferromagnet $Fe_{0.47}Zn_{0.53}F_2$.[24] The scaling invariant power law hints at a wide size distribution and, probably, fractality of the final nanoclusters involved. Indeed, the decay of large initial domains into RF correlated dynamic ones at $T>T_c$ is governed by activated cluster flips on many length scales. This is corroborated by the failure of a KWW fit for these data, which is expected to hold only for final stage domain-wall relaxation in the very long time limit.

Obviously, the smoothing of antiferromagnetic domains in FeF_2:Zn and the roughening of the ferroelectric single domain in SBN:Ce are both controlled by the same kinetics. This emphasizes that quenched RF's might be at the origin of the nanocluster formation in the high-temperature relaxor phase. Remarkably, exactly the same relaxation laws as those found on SBN:Ce were reported for PMN in field-induced linear birefringence measurements.[25] After stepwise changes of an external electric field the autocorrelation function $\langle P^2\rangle$ varies power law and stretched exponential-like in the paraelectric and ferroelectric regimes, respectively.

Figure 4(a) shows the spatial distribution of the zero-field-cooled polarization at room temperature in binary contrast. According to the results of the temporal relaxation (Fig. 3) the initial paraelectric state was prepared by keeping the sample at $T=350\,\mathrm{K}$ for approximately 3×10^5 s. Upon cooling the sample to below T_C within about 10^3 s the domain pattern evolving in the vicinity of T_C was frozen in its initial state. The black-and-white pattern shows irregular patches of either ''color'' on various length scales. There are large uniform areas with fuzzy borders, splitting off small patches to both sides (''domains in domains'').[26] The inset of Fig. 4(c) represents the surface of one typical domain extracted by computer out of the domain pattern in Fig. 4(a) (gray col-

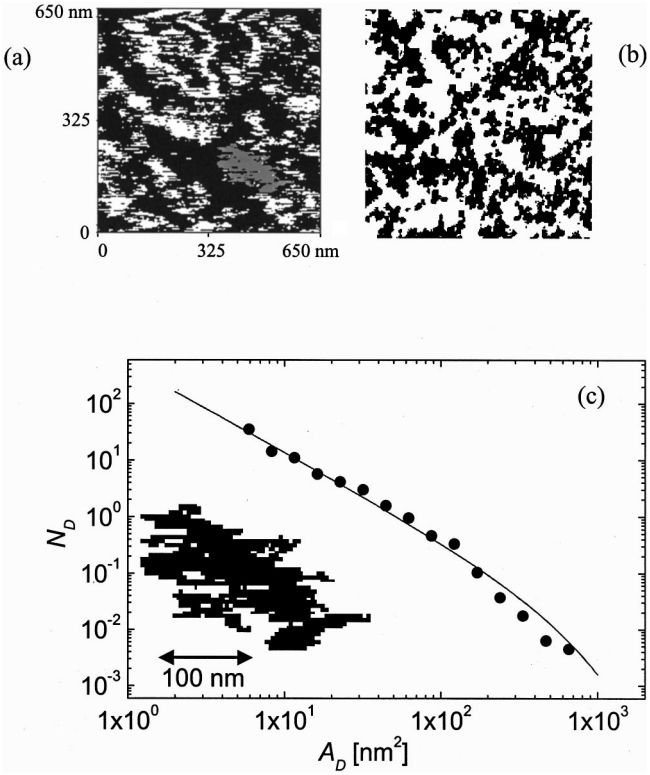

FIG. 4. (a) Spatial distribution of the zero-field-cooled surface polarization and (b) obtained from MC simulation,[27] respectively. (c) Logarithmic averaged number of domains N_D with size A_D plotted versus A_D. The solid line represents the fit to Eq. (1). The inset shows the extracted gray-colored single domain from (a).

ored). Its shape reminds of fractal objects similar as those found in Monte Carlo (MC) simulations of the 3D RFIM.[26,27] Figure 4(b) shows the surface of a typical domain pattern out of a simulated 3D RFIM system after RF cooling to below T_C.[27] Similarity with the pattern obtained on SBN:Ce in Fig. 4(a) seems obvious, although the third dimension and the fine structure on an atomic scale are not provided by the PFM technique.

Similar results were obtained from high-resolution transmission electron-microscopy (HRTEM) measurements on SBN.[28,29] However, an incommensurate structure with modulations of the intraplanar lattice constant was reported for SBN.[30] Thus, the ''domains'' visualized by HRTEM are expected to reflect the incommensurate strain pattern in addition to the polar structure. For this reason PFM might be considered more adequate for viewing exclusively the polar structure of the sample.

The domain-size distribution of the domain pattern [Fig. 4(b)] is well described by a power law with exponential cutoff[31]

$$N_D(A_D) \propto A_D^{-\delta} \exp(-A_D/A_0). \quad (1)$$

The areas A_D of the domains were determined by counting the pixels using the image-processing software GLOBAL LAB Image (Data Translation, Inc.). The best-fit of Eq. (1) to our data [solid line in Fig. 4(c)] yields an exponent $\delta = 1.53 \pm 0.13$, which complies with that of the 2D RFIM in the limit of strong RF's, where $\delta = 1.55$ is expected.[32] This result seems to reflect that the PFM merely measures a projection of the 3D domain pattern in the vicinity of the surface.[22] Data on the volume-distribution function of the domains would be needed to verify the value expected for the 3D RFIM, $\delta = 1.8$.[31]

The evaluation of Fig. 4(a) yields the cutoff size $A_0 = 5280 \pm 9750\ \mathrm{nm}^2$. The large error is due to the insufficient statistics provided by the small domain number, $\Sigma N_j \approx 300$. Further experiments on samples with different concentrations of Ce^{3+} and better statistics have to be done in order to clarify the RF dependence of A_0.

IV. CONCLUSION

One key issue in understanding relaxor behavior is the mechanism of polar-cluster formation. In the case of the uniaxial system SBN:Ce our experimental results strongly suggest quenched RF's to provide the microscopic mechanism. Roughening of 180° domain walls indicates the thermally driven decay into a nanodomain state, which is quasistatic close to and even above T_C. Isothermal relaxation of field-cooled macrodomains shows a stretched exponential decay into a RF-induced domain state, whereas a decay of power law type into a multicluster state is observed above T_C. Fractal-like nanodomains are characteristic for the zero-field-cooled state and are observed for the first time with PFM in SBN. Their size-distribution fits well to a power law with an exponential cutoff as predicted from computer experiments.

The RF-dependence of the cutoff size is the aim of further experiments and is expected to decrease with increasing RF's viz. Ce^{3+} concentration. In addition, future experiments with higher spatial resolution have to be done in order to study the domain nucleation upon cooling to below T_C and to investigate the fractality of the domain walls.

ACKNOWLEDGMENTS

This research was supported by the Deutsche Forschungsgemeinschaft within the framework of the Schwerpunktprogramm ''Strukturgradienten in Kristallen.'' Useful discussions with J. Dec and U. Nowak are gratefully acknowledged. Thanks are due to M. Aderholz for the development of the hot stage for the scanning-probe microscope.

[1] L. E. Cross, Ferroelectrics **76**, 241 (1987); **151**, 305 (1994).
[2] G. A. Smolenskii and V. A. Isupov, Dokl. Akad. Nauk SSSR **9**, 653 (1954).
[3] A. M. Glass, J. Appl. Phys. **40**, 4699 (1969).
[4] D. Viehland, S. J. Jang, L. E. Cross, and M. Wuttig, J. Appl. Phys. **68**, 847 (1990).
[5] N. de Mathan, E. Husson, G. Calvarin, J. R. Gavarri, A. W. Hewat, and A. Morell, J. Phys.: Condens. Matter **3**, 8159 (1991).

[6] R. Blinc, J. Dolinsek, A. Gregorovic, B. Zalar, C. Filipic, Z. Kutnjak, A. Levstik, and R. Pirc, Phys. Rev. Lett. **83**, 424 (1999); R. Pirc and R. Blinc, Phys. Rev. B **60**, 13 470 (1999).
[7] Chen Ang, Zhi Yu, and Zhi Jing, Phys. Rev. B **61**, 957 (2000).
[8] W. Kleemann, V. Bobnar, J. Dec, P. Lehnen, R. Pankrath, and S. A. Prosandeev, Ferroelectrics (to be published).
[9] I. Imry and S. K. Ma, Phys. Rev. Lett. **35**, 1399 (1975).
[10] A. Aharony, Solid State Commun. **29**, 607 (1978).
[11] V. Westphal, W. Kleemann, and M. D. Glinchuk, Phys. Rev. Lett. **68**, 847 (1992); W. Kleemann, Int. J. Phys. B **7**, 2469 (1993).
[12] J. Dec, W. Kleemann, Th. Woike, and R. Pankrath, Eur. Phys. J. B **14**, 627 (2000).
[13] P. Lehnen, W. Kleemann, Th. Woike, and R. Pankrath, Eur. Phys. J. B **14**, 633 (2000).
[14] W. Kleemann, J. Dec, P. Lehnen, Th. Woike, and R. Pankrath, in *Fundamental Physics of Ferroelectrics 2000*, edited by R. E. Cohen, AIP Conf. Proc. No. 535 (AIP, Melville, NY, 2000), p. 26.
[15] D. P. Belanger and A. P. Young, J. Magn. Magn. Mater. **100**, 272 (1991).
[16] Y.-G. Wang, W. Kleemann, Th. Woike, and R. Pankrath, Phys. Rev. B **61**, 3333 (2000).
[17] Y.-G. Wang, J. Dec, and W. Kleemann, J. Appl. Phys. **84**, 6795 (1998).
[18] P. Lehnen, J. Dec, and W. Kleemann, J. Phys. D **33**, 1932 (2000).
[19] H. Birk, J. Glatz-Reichenbach, Li-Jie, E. Schreck, and K. Dransfeld, J. Vac. Sci. Technol. B **9**, 1162 (1991); P. Güthner and K. Dransfeld, Appl. Phys. Lett. **61**, 1137 (1992).
[20] K. Franke, J. Besold, W. Haessler, and C. Seegebarth, Surf. Sci. Lett. **302**, L283 (1994); K. Franke, Ferroelectr. Lett. Sect. **19**, 25 (1995).
[21] P. Lehnen, E. Beckers, W. Kleemann, Th. Woike, and R. Pankrath, Ferroelectrics **253**, 11 (2001).
[22] H.-J. Ding, P.-F. Hou, and F.-L. Guo, Int. J. Solids Struct. **37**, 3201 (2000).
[23] T. Granzow, U. Dörfler, Th. Woike, M. Wöhlecke, R. Pankrath, M. Imlau, and W. Kleemann, Phys. Rev. B **63**, 174101 (2001).
[24] S.-J. Han, D. P. Belanger, W. Kleemann, and U. Nowak, Phys. Rev. B **45**, 9728 (1992).
[25] W. Kleemann and R. Lindner, Ferroelectrics **199**, 1 (1997).
[26] J. L. Cambier and M. Nauenberg, Phys. Rev. B **34**, 7998 (1986).
[27] U. Nowak, Fractals **1**, 992 (1993).
[28] L. A. Bursill and P. J. Lin, Philos. Mag. A **54**, 157 (1986).
[29] W.-H. Huang, Z. Xu, and D. Viehland, Philos. Mag. A **71**, 219 (1995).
[30] J. Schneck, J. C. Toledano, R. Whatmore, and F. W. Ainger, Ferroelectrics **36**, 327 (1981).
[31] U. Nowak, J. Esser, and K. D. Usadel, Physica A **232**, 40 (1996).
[32] J. Esser, U. Nowak, and K. D. Usadel, Phys. Rev. B **55**, 5866 (1997).